

# The kinks, the solitons and the shocks in series connected discrete Josephson transmission lines

Eugene Kogan<sup>1,\*</sup>

<sup>1</sup>*Department of Physics, Bar-Ilan University, Ramat-Gan 52900, Israel*

(Dated: April 15, 2022)

We analytically study the localized running waves in the discrete Josephson transmission lines (JTL), constructed from Josephson junctions (JJ) and capacitors. The quasi-continuum approximation reduces calculation of the running wave properties to the problem of equilibrium of an elastic rod in the potential field. Making additional approximation, we reduce the problem to the motion of the fictitious Newtonian particle in the potential well. We show that there exist running waves in the form of supersonic kinks and solitons and calculate their velocities and profiles. We show that the nonstationary smooth waves which are small perturbations on the homogeneous non-zero background are described by Korteweg-de Vries equation, and those on zero background – by modified Korteweg-de Vries equation. We also study the effect of dissipation on the running waves in JTL and find that in the presence of the resistors, shunting the JJ and/or in series with the ground capacitors, the only possible stationary running waves are the shock waves, whose profiles are also found.

PACS numbers:

## I. INTRODUCTION

The concept that in a nonlinear wave propagation system the various parts of the wave travel with different velocities, and that wave fronts (or tails) can sharpen into shock waves, is deeply imbedded in the classical theory of fluid dynamics<sup>1</sup>. The methods developed in that field can be profitably used to study signal propagation in nonlinear transmission lines<sup>2–11</sup>. In the early studies of shock waves in transmission lines, the origin of the nonlinearity was due to nonlinear capacitance in the circuit<sup>12–14</sup>.

Interesting and potentially important examples of nonlinear transmission lines are circuits containing Josephson junctions (JJ)<sup>15</sup> – Josephson transmission lines (JTL)<sup>16–19</sup>. The unique nonlinear properties of JTL allow to construct soliton propagators, microwave oscillators, mixers, detectors, parametric amplifiers, and analog amplifiers<sup>17–19</sup>.

Transmission lines formed by JJ connected in series were studied beginning from 1990s, though much less than transmission lines formed by JJ connected in parallel<sup>20</sup>. However, the former began to attract quite a lot of attention recently<sup>21–28</sup>, especially in connection with possible JTL traveling wave parametric amplification<sup>29–31</sup>.

The interest in studies of discrete nonlinear electrical transmission lines, in particular of lossy nonlinear transmission lines, has started some time ago<sup>32–34</sup>, but it became even more pronounced recently<sup>35–37</sup>. These studies should be seen in the general context of waves in strongly nonlinear discrete systems<sup>38–44</sup>.

In our previous publication<sup>45</sup> we considered shock waves in the continuous JTL with resistors, studying the influence of those on the shock profile. Now we want to analyse wave propagation in the discrete JTL, both lossless and lossy.

The rest of the paper is constructed as follows. In Sec-

tion II we formulate the approximation to the circuit equations of the discrete lossless JTL. In Section III we formulate the quasi-continuum approximation and show the analogy between the problem of the running waves and the problem of equilibrium of an elastic rod in the potential field. In Section IV, by simplifying the approximation, we reduce the problem of the running waves to an effective mechanical problem, describing motion of a fictitious particle in a potential well and study the profiles of the kinks and of the solitons. In Section V we consider specifically weak kinks and weak solitons. In Section VI we formulate the modified quasi-continuum approximation and, on top of it, the simple wave approximation, which opens the way to conveniently study non-stationary waves in the JTL. In Section VII we discuss the effect of dissipation on the running waves in the discrete JTL. In Section VIII we briefly mention possible applications of the results obtained in the paper and opportunities for their generalization. We conclude in Section IX. In the Appendix A we apply the modified quasi-continuum approximation to the discrete linear transmission line. In the Appendix B we propose the integral approximation to the discrete transmission lines equations.

## II. THE DISCRETE JOSEPHSON TRANSMISSION LINE

Consider the model of JTL constructed from identical JJ and capacitors, which is shown on Fig. 1. We take as dynamical variables the phase differences (which we for brevity will call just phases)  $\varphi_n$  across the JJ and the charges  $q_n$  which have passed through the JJ. The circuit

equations are

$$\frac{\hbar}{2e} \frac{d\varphi_n}{dt} = \frac{1}{C} (q_{n+1} - 2q_n + q_{n-1}) , \quad (1a)$$

$$\frac{dq_n}{dt} = I_c \sin \varphi_n , \quad (1b)$$

where  $C$  is the capacitor, and  $I_c$  is the critical current of the JJ. Differentiating Eq. (1a) with respect to  $t$  and substituting  $dq_n/dt$  from Eq. (1b), we obtain closed equation for  $\varphi_n$

$$\frac{\partial^2 \varphi}{\partial \tau^2} = \sin \varphi_{n+1} - 2 \sin \varphi_n + \sin \varphi_{n-1} , \quad (2)$$

where we have introduced the dimensionless time  $\tau = t/\sqrt{L_J C}$ .

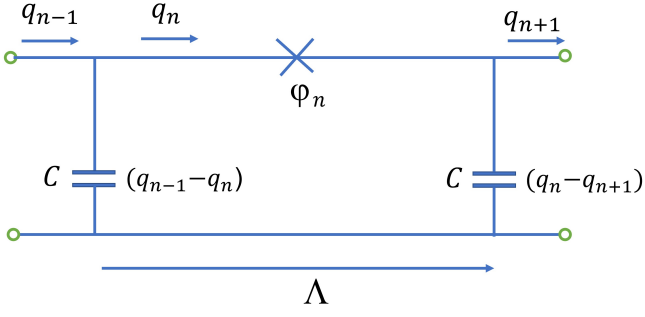


FIG. 1: Discrete JTL.

It is interesting to compare Eq. (2) with a discretized  $\phi^4$  theory<sup>46</sup>

$$\frac{d^2 \phi_n}{d\tau^2} = \frac{1}{h^2} (\phi_{n+1} - 2\phi_n + \phi_{n-1}) + 2\phi_n (1 - \phi_n^2) , \quad (3)$$

and a discrete sine-Gordon equation for lattice wave field<sup>42</sup>

$$\frac{d^2 \varphi_n}{d\tau^2} - D(\varphi_{n+1} - 2\varphi_n + \varphi_{n-1}) + \sin \varphi_n = 0 . \quad (4)$$

where  $h$  and  $D$  are some constants. Comparing Eqs. (3) and (4) with (2), one realizes, that for the JTL the non-linearity enters into the problem in a totally different way. We'll see later that our problem has an additional free parameter – the amplitude of the wave, which, in particular, opens the way for the controlled perturbation theory.

Let us return to Eq. (1). The kinks, we'll be interested in, are localized and characterised by the boundary conditions

$$\lim_{n \rightarrow -\infty} \varphi = \varphi_2 , \quad \lim_{n \rightarrow +\infty} \varphi = \varphi_1 . \quad (5)$$

Summing up (1a) from far to the left of the kink up to far to the right of the kink we obtain

$$\frac{\hbar}{2e} \frac{d}{dt} \sum_n \varphi_n = \frac{1}{C} [(q_{n+1} - q_n)_1 - (q_{n+1} - q_n)_2] . \quad (6)$$

Further on in this paper, instead of the index  $n$  will use a continuous variables  $z = n\Lambda$  and will be mostly interested in the running wave solutions of the form

$$\varphi(z, t) = \varphi(x) , \quad q(z, t) = q(x) , \quad (7)$$

where  $x = Ut - z$ , and  $U$  is the running wave velocity. The boundary conditions become

$$\lim_{x \rightarrow -\infty} \varphi = \varphi_1 , \quad \lim_{x \rightarrow +\infty} \varphi = \varphi_2 . \quad (8)$$

From the running wave ansatz follows

$$\frac{d}{dt} \sum_n \varphi_n = \frac{U}{\Lambda} (\varphi_1 - \varphi_2) . \quad (9)$$

To deal with the r.h.s. of (6) we need to approximate the finite difference only far away from the kink, where everything changes slowly, and the continuum approximation

$$q_{n+1} - q_n = \Lambda \frac{\partial q}{\partial z} \quad (10)$$

is enough. From (10) and the running wave ansatz follows

$$(q_{n+1} - q_n)_i = \frac{\Lambda}{U} \left( \frac{dq_n}{dt} \right)_i = \frac{\Lambda}{U} \sin \varphi_i . \quad (11)$$

Substituting (9) and (11) into (6) we get for the running wave velocity

$$\bar{U}^2 = \frac{\sin \varphi_1 - \sin \varphi_2}{\varphi_1 - \varphi_2} \equiv \bar{U}_{\text{sh}}^2(\varphi_1, \varphi_2) . \quad (12)$$

In this paper, for any velocity  $V$ ,  $\bar{V} \equiv V \sqrt{L_J C} / \Lambda$ , and  $L_J = \hbar / (2eI_c)$ . The reason, why we have chosen subscript sh for the velocity in (12), will become clear in Section VII.

To find the profile of the running wave we have to approximate the finite difference in the r.h.s. of (1a) everywhere, including the regions where the variables change fast. We can write down (at least formally) the infinite Taylor expansion

$$q_{n+1} - 2q_n + q_{n-1} = \Lambda^2 \frac{\partial^2 q}{\partial z^2} + \frac{\Lambda^4}{12} \frac{\partial^4 q}{\partial z^4} + \dots \quad (13)$$

For the running waves, substituting into the r.h.s. of (13) the derivative of  $q$  with respect to  $z$  from (1b) and then substituting the result into (1a), we obtain the ordinary differential equation

$$\bar{U}^2 \frac{d\varphi}{dx} = \frac{d \sin \varphi}{dx} + \frac{\Lambda^2}{12} \frac{d^3 \sin \varphi}{dx^3} + \dots \quad (14)$$

Integrating with respect to  $x$  we obtain

$$\frac{\Lambda^2}{12} \frac{d^2 \sin \varphi}{dx^2} + \dots = -\sin \varphi + \bar{U}^2 \varphi + F , \quad (15)$$

where  $F$  is the constant of integration. Substituting (8) into (15) we obtain

$$-\sin \varphi_i + \bar{U}^2 \varphi_i + F = 0, \quad i = 1, 2. \quad (16)$$

Solving (16) relative to  $\bar{U}^2$  and  $F$  we recover (12) and also obtain

$$F = \frac{\varphi_1 \sin \varphi_2 - \varphi_2 \sin \varphi_1}{\varphi_1 - \varphi_2}. \quad (17)$$

### III. THE ELASTICITY THEORY: THE KINKS AND THE SOLITONS

Now we make the assumption, by keeping in Eq. (13) only the first three terms

$$q_{n+1} - 2q_n + q_{n-1} = \Lambda^2 \frac{\partial^2 q}{\partial z^2} + \frac{\Lambda^4}{12} \frac{\partial^4 q}{\partial z^4} + \frac{\Lambda^6}{360} \frac{\partial^6 q}{\partial z^6}. \quad (18)$$

We will call (18) the quasi-continuum approximation. We have seen above that the terms with the derivatives higher than the second are necessary to obtain a physically meaningful results. On the other hand, the term with the 6th derivative is necessary so the Eq. (2) after the truncation

$$\frac{\partial^2 \varphi}{\partial \tau^2} = \Lambda^2 \frac{\partial^2 \sin \varphi}{\partial z^2} + \frac{\Lambda^4}{12} \frac{\partial^4 \sin \varphi}{\partial z^4} + \frac{\Lambda^6}{360} \frac{\partial^6 \sin \varphi}{\partial z^6} \quad (19)$$

would be non-singular at small wavelengths.

Introducing the notation  $y = \sin \varphi$ , we write down Eq. (15) after the truncation as

$$\frac{\Lambda^4}{360} y^{(IV)} + \frac{\Lambda^2}{12} y'' = -y + \bar{U}^2 \sin^{-1} y + F. \quad (20)$$

We recognize the equation of equilibrium of bent and compressed rods for the case of small deflections<sup>47</sup>,  $\Lambda^4/360$  playing the role of the bending modulus and  $\Lambda^2/12$  playing the role of the compressing force. The rod is placed in the external force field, described alternatively by the potential energy  $\Pi(y)$  given by (27).

One important feature of the solutions of (20) can be seen without solving the equation: the localized solutions at the infinite line with the boundary conditions (8) and the finite energy exist only if

$$\varphi_2 = \pm \varphi_1. \quad (21)$$

If  $\varphi_2 = -\varphi_1$  we can talk about the kinks, if  $\varphi_2 = \varphi_1$  – about the solitons.

In fact, we know that the solutions of (20) may be obtained from the variational principle<sup>47</sup>. We have to make stationary the functional

$$F_{\text{rod}} = \frac{\Lambda^4}{720} \int y''^2 dx - \frac{\Lambda^2}{24} \int y'^2 dx + \int \Pi(y) dx. \quad (22)$$

The variational principle being formulated, we immediately understand the necessity of the relation

$$\Pi(\varphi_1) = \Pi(\varphi_2), \quad (23)$$

Otherwise, by shifting the kink or the soliton we can change the functional linearly with respect to the shift. Combining (23) with (16) we obtain (21).

### IV. NEWTONIAN EQUATION: THE KINKS AND THE SOLITONS

Let us simplify Eq. (18) to

$$q_{n+1} - 2q_n + q_{n-1} = \Lambda^2 \frac{\partial^2 q}{\partial z^2} + \frac{\Lambda^4}{12} \frac{\partial^4 q}{\partial z^4}. \quad (24)$$

We will call (24) the reduced quasi-continuum approximation and will see later that in certain limiting cases it can be rigorously justified. After the simplification, Eq. (20) reduces to

$$\frac{\Lambda^2}{12} \frac{d^2 \sin \varphi}{dx^2} = -\sin \varphi + \bar{U}^2 \varphi + F. \quad (25)$$

We can consider  $x$  as time and  $\sin \varphi$  as the coordinate of the fictitious particle, visualizing (25) as Newtonian equation. Thus the problem of finding the profile of the kink is reduced to studying the motion of the particle which starts from an equilibrium position, and ends in an equilibrium position.

Multiplying Eq. (25) by the integrating multiplier  $d \sin \varphi / dx$  and integrating once again we obtain

$$\frac{\Lambda^2}{24} \left( \frac{d \sin \varphi}{dx} \right)^2 + \Pi(\sin \varphi) = E, \quad (26)$$

where

$$\Pi(\sin \varphi) = \frac{1}{2} \sin^2 \varphi - \bar{U}^2 (\varphi \sin \varphi + \cos \varphi) - F \sin \varphi, \quad (27)$$

and  $E$  is another constant of integration. Using the expertise we acquired in mechanics classes, we come to the conclusion that the initial position corresponds to maxima of the "potential energy"  $\Pi(\sin \varphi)$ , and so does the final position. Note that from the energy conservation law we recover (23) and, hence, (21).

One should compare the kink velocity with the velocity  $u(\varphi)$  of propagation along the JTL of small amplitude smooth disturbances of phase on a homogeneous background  $\varphi$ <sup>45</sup>

$$\bar{u}^2(\varphi) = \cos \varphi \quad (28)$$

(in this paper we consider only the solutions which lie completely in the sector  $(-\pi/2, \pi/2)$ .) From the fact

that there is a maximum of the "potential energy" at the points  $\varphi_{1,2}$ , follows that

$$\frac{d^2\Pi(\varphi)}{d\varphi^2}\Big|_{\varphi=\varphi_{1,2}} < 0. \quad (29)$$

Calculating the derivatives we obtain

$$\bar{U}^2 > \cos \varphi_{1,2}, \quad (30)$$

that is the running wave is supersonic.

Adding the energy conservation law to (16) we obtain

$$F = 0, \quad (31a)$$

$$\bar{U}^2 = \bar{U}_{\text{sh}}^2(\varphi_1, -\varphi_1) = \frac{\sin \varphi_1}{\varphi_1} \equiv \bar{U}_{\text{k}}^2(\varphi_1), \quad (31b)$$

and, after the substitution into (27),

$$\Pi(\sin \varphi) = \frac{1}{2}(\sin \varphi - \sin \varphi_1)^2 - \frac{\sin \varphi_1}{\varphi_1}[\cos \varphi - \cos \varphi_1 - (\varphi_1 - \varphi) \sin \varphi] \quad (32)$$

(and  $E = 0$ ). The "potential energy" (32) is graphically presented on Fig. 2 (above), and the kink profile – on Fig. 2 (below).

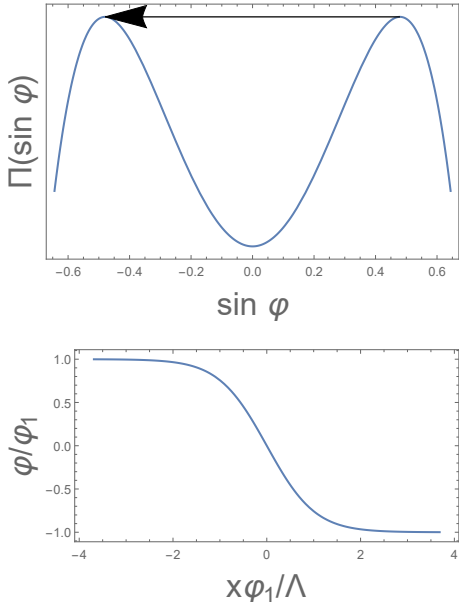


FIG. 2: The "potential energy" (32) (above) and the kink profile calculated with this energy according to Eq. (26) (below). We have chosen  $\varphi_1 = .5$ .

For the case of the soliton, the two maxima of the potential energy mentioned after Eq. (27) are the same maximum, that is the particle returns to the initial position after reflection from a potential wall (see Fig. 3). Note that due to exactly the same reasons as given in the previous Section for the kink, the soliton is also supersonic. In this case the two equations of (16) become one

equation. As an additional parameter we take the amplitude of the soliton (maximally different from  $\varphi_1$  value of  $\varphi$ ), which we will designate as  $\varphi_0$ . Adding to (16) the equation

$$\Pi(\sin \varphi_0) = \Pi(\sin \varphi_1) \quad (33)$$

and solving the obtained system we obtain

$$\bar{U}_{\text{sol}}^2(\varphi_1, \varphi_0) = \frac{(\sin \varphi_1 - \sin \varphi_0)^2}{2[\cos \varphi_0 - \cos \varphi_1 - (\varphi_1 - \varphi_0) \sin \varphi_0]}, \quad (34a)$$

$$\Pi(\sin \varphi) = \frac{1}{2}(\sin \varphi_1 - \sin \varphi)^2 - \bar{U}_{\text{sol}}^2(\varphi_1, \varphi_0) \cdot [\cos \varphi - \cos \varphi_1 - (\varphi_1 - \varphi) \sin \varphi] \quad (34b)$$

(and  $E = 0$ ). Note that while derivation of the formula for the kink velocity demands approximation of the wave behavior only far away from the kink, derivation of the formula for the soliton velocity demands approximation of the wave behaviour in the region of the soliton. The "potential energy" (34b) is graphically presented on Fig. 3 (above), and the soliton profile – on Fig. 3 (below).

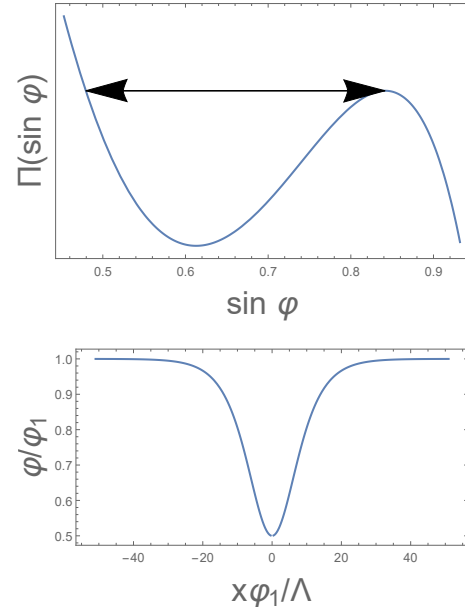


FIG. 3: The "potential energy" (34b) (above) and the soliton profile according to Eq. (26) (below). We have chosen  $\varphi_1 = 1$  and  $\varphi_0 = .5$ .

## V. WEAK KINKS AND WEAK SOLITONS

Consider specifically the limiting case of weak kinks ( $|\varphi_1| \ll 1$ ). Expanding the "potential energy" with respect to  $\varphi$  and  $\varphi_1$  and keeping only the lowest order terms we obtain the approximation to Eq. (26) in the form

$$\Lambda^2 \left( \frac{d\varphi}{dx} \right)^2 = (\varphi_1^2 - \varphi^2)^2. \quad (35)$$

The solution of Eq. (35) is

$$\varphi(x) = -\varphi_1 \tanh \frac{\varphi_1 x}{\Lambda}. \quad (36)$$

Equations (36) coincides with that obtained by Katayama et al.<sup>36</sup>. So does Eq. (31b), being expanded in series with respect to  $\varphi_1$  and truncated after the first two terms:

$$\bar{U}_k(\varphi_1) = 1 - \frac{\varphi_1^2}{6}. \quad (37)$$

In the limiting case of weak solitons ( $\Delta\varphi \tan \varphi_1 \ll 1$ ,  $\varphi_1 \sim 1$ , where  $\Delta\varphi \equiv \varphi_1 - \varphi_0$ ), it is convenient to make the change of variable  $\psi \equiv \varphi - \varphi_1$ , after which Eq. (26) takes the form

$$\Lambda^2 \left( \frac{d\psi}{dx} \right)^2 = 4 \tan \varphi_1 \cdot \psi^2 (\psi + \Delta\varphi). \quad (38)$$

The solution of Eq. (38) is

$$\psi = -\Delta\varphi \operatorname{sech}^2 \left( \sqrt{\Delta\varphi \tan \varphi_1} x / \Lambda \right). \quad (39)$$

Velocity of the soliton in this approximation is

$$\bar{U}_{\text{sol}}^2(\varphi_1, \varphi_0) = \cos \varphi_1 \left( 1 + \frac{\tan \varphi_1}{3} \Delta\varphi \right). \quad (40)$$

Looking at Eqs. (36) and (39) we realize with the hindsight that the reduced quasi-continuum approximation can be rigorously justified when the running wave is a small perturbation on a homogeneous background. Actually, the equations say more than that. Common wisdom says that the continuum approximation and the small amplitude approximation are independent - there could be a wave with small amplitude, which allows to expand the sine function, but which varies fast in space (wavelength comparable to lattice spacing), so the continuum limit is not justified. And there could be the opposite situation (large amplitude, long wavelength), in which the sine needs to be retained but the continuum limit is allowed.

However, for the running waves in the discrete JTL these approximations are not independent. Parametrically, the length scale of the waves is of the order of the lattice spacing  $\Lambda$ , so, naively, the quasi-continuum approximation can not be justified. What we have shown above, is that for the weak kinks the length scale is  $\Lambda/|\varphi_1|$ , and for the weak solitons the length scale is  $(\Lambda/\sqrt{|\Delta\varphi|})$ , thus justifying the reduced quasi-continuum approximation in both cases.

## VI. THE SIMPLE WAVE APPROXIMATION

Let us modify the quasi-continuum approximation (18) in the following way

$$q_{n+1} - 2q_n + q_{n-1} = \left( \Lambda \frac{\partial}{\partial z} + \frac{\Lambda^3}{24} \frac{\partial^3}{\partial z^3} \right)^2 q. \quad (41)$$

After we apply the modified quasi-continuum approximation to the r.h.s. of Eq. (1a), Eq. (2) is modified to

$$\frac{\partial^2 \varphi}{\partial \tau^2} = \left( \Lambda \frac{\partial}{\partial z} + \frac{\Lambda^3}{24} \frac{\partial^3}{\partial z^3} \right)^2 \sin \varphi. \quad (42)$$

This modification opens the way for the simple wave approximation, that is decoupling of the wave equation into two separate equations for the right- and left-going waves. Such decoupling can be easily done for the linear wave equations, as it is shown in Appendix A. Following the pattern, let us decouple (42) into 2 equations for  $|\varphi| \ll 1$  by brute force as

$$\frac{\partial \varphi}{\partial \tau} = \pm \left( \Lambda \frac{\partial}{\partial z} + \frac{\Lambda^3}{24} \frac{\partial^3}{\partial z^3} \right) \sqrt{\frac{\sin \varphi}{\varphi}} \varphi. \quad (43)$$

Taking

$$\sqrt{\frac{\sin \varphi}{\varphi}} = 1 - \frac{\varphi^2}{12}, \quad (44)$$

substituting (44) into (42) and keeping only the leading terms we obtain the equations

$$\frac{\partial \varphi}{\partial \tau} = \pm \left( \Lambda \frac{\partial \varphi}{\partial z} - \frac{\Lambda}{12} \frac{\partial \varphi^3}{\partial z} + \frac{\Lambda^3}{24} \frac{\partial^3 \varphi}{\partial z^3} \right), \quad (45)$$

which are modified Korteweg-de Vries (mKdV) equations<sup>36</sup>.

When  $\varphi = \psi + \varphi_1$  ( $|\psi| \ll 1$ ,  $\varphi_1 \sim 1$ ), we present  $\sin \varphi$  (ignoring the  $\psi$ -independent term) as

$$\sin \varphi = \cos \varphi_1 \left( 1 - \frac{\tan \varphi_1}{2} \psi \right) \psi, \quad (46)$$

substitute into (42), extract the square root, taking into account that as

$$\left( 1 - \frac{\tan \varphi_1}{2} \psi \right)^{1/2} = 1 - \frac{\tan \varphi_1}{4} \psi, \quad (47)$$

and keep only the leading terms to obtain

$$\frac{\partial \psi}{\partial \tau} = \pm \sqrt{\cos \varphi_1} \left( \Lambda \frac{\partial \psi}{\partial z} - \frac{\tan \varphi_1}{4} \Lambda \frac{\partial \psi^2}{\partial z} + \frac{\Lambda^3}{24} \frac{\partial^3 \psi}{\partial z^3} \right), \quad (48)$$

which is Korteweg-de Vries (KdV) equation.

Equations (45) and (48) were derived to solve nonstationary problems, but they also can be conveniently used for describing the running waves, in which case the equations take the form (after being integrated once)

$$\frac{\Lambda^2}{24} \frac{d^2 \varphi}{dx^2} = (\bar{U} - 1) \varphi + \frac{1}{12} \varphi^3 + F, \quad (49)$$

and

$$\frac{\Lambda^2}{24} \frac{d^2 \psi}{dx^2} = (\bar{U} / \sqrt{\cos \varphi_1} - 1) \psi + \frac{\tan \varphi_1}{4} \psi^2 + F. \quad (50)$$

From the boundary conditions (8) for the kink, and from the boundary condition (8) and the energy conservation law (33) for the soliton, we obtain  $F = 0$  and

$$\bar{U}_k = 1 - \frac{\varphi_1^2}{12}, \quad (51)$$

and

$$\bar{U}_{\text{sol}} = \sqrt{\cos \varphi_1} \left( 1 + \frac{\tan \varphi_1}{6} \Delta \varphi \right), \quad (52)$$

which coincides (for the approximation used) with (37) and (40). Integrating (49) and (50) we recover (35) and (38).

## VII. THE SHOCKS

Consider JTL with the capacitor and resistor shunting the JJ and another resistor in series with the ground capacitor, shown on Fig. 4. As the result, Eq. (1) changes to

$$\frac{\hbar}{2e} \frac{d\varphi_n}{dt} = \left( \frac{1}{C} + R \frac{\partial}{\partial t} \right) (q_{n+1} - 2q_n + q_{n-1}), \quad (53a)$$

$$\frac{dq_n}{dt} = I_c \sin \varphi_n + \frac{\hbar}{2eR_J} \frac{d\varphi_n}{dt} + C_J \frac{\hbar}{2e} \frac{d^2\varphi_n}{dt^2}, \quad (53b)$$

where  $R$  is the ohmic resistor in series with the ground capacitor, and  $C_J$  and  $R_J$  are the capacitor and the ohmic resistor shunting the JJ.

Considering again the running wave solutions we obtain the generalization of Eq. (25)

$$\begin{aligned} \frac{\Lambda^2}{12} \frac{d^2 \sin \varphi}{dx^2} + \left( \frac{C_J}{C} + \frac{R}{R_J} \right) \bar{U}^2 \Lambda^2 \frac{d^2 \varphi}{dx^2} \\ + \left( \frac{R}{Z_J} \cos \varphi + \frac{Z_J}{R_J} \right) \bar{U} \Lambda \frac{d\varphi}{dx} = -\sin \varphi + \bar{U}^2 \varphi + F, \end{aligned} \quad (54)$$

where  $Z_J \equiv \sqrt{L_J/C}$  is the characteristic impedance of the JTL, and we discarded the terms with the derivatives higher than of the forth order.

We impose the boundary conditions (8) and try to understand what part of the analysis of Section IV can be transferred to the present case. The results (16) are determined only by the r.h.s. of Eq. (25), so are (14), following from (16). Since the r.h.s. of Eqs. (25) and (54) are identical, these equations are valid in the present case also. In particular, we obtain

$$\bar{U}^2 = \bar{U}_{\text{sh}}^2(\varphi_1, \varphi_2). \quad (55)$$

On the other hand, the resistors, by introducing the effective "friction force", break the "energy" conservation law, which means that the stationary kinks and the solitons we considered previously are no longer possible, however weak the dissipation is. However in the lossy JTL the solutions with  $|\varphi_2| \neq |\varphi_1|$  (the shocks) are possible.

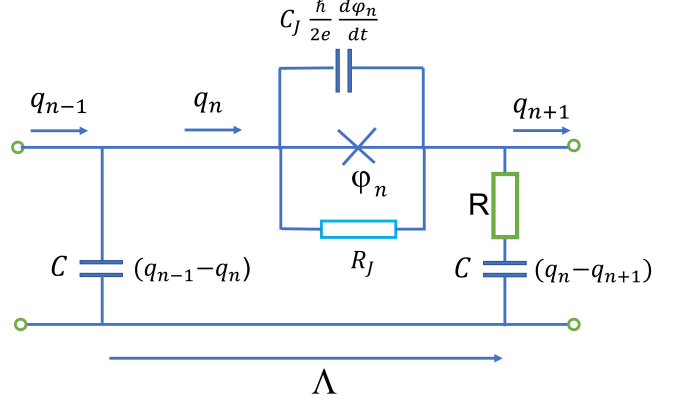


FIG. 4: Discrete JTL with the capacitor and the resistor shunting the JJ and another resistor in series with the ground capacitor

### A. The qualitative analysis

We saw in Section IV that if

$$\left( \frac{C_J}{C} + \frac{R}{R_J} \right) \bar{U}^2 \ll 1, \quad (56)$$

Eq. (54) can be reduced to Newtonian form. The situation is even simpler when the inequality (56) is inverted. In this case the first term in the l.h.s. of (54) can be neglected, and the equation is already in Newtonian form. In the latter case the discrete nature of the JTL doesn't manifest itself – the continuum approximation is valid<sup>45</sup>. In each of these cases, the fictitious particle motion describing the shock connects the "potential energy" maximum at  $\varphi = \varphi_1$  with the "potential energy" minimum at  $\varphi = \varphi_2$ . Thus in the continuum approximation and for weak shocks ( $|\varphi_1 - \varphi_2| \ll |\varphi_1|$ ), Eq. (54) simplifies to

$$\begin{aligned} \left( \frac{C_J}{C} + \frac{R}{R_J} \right) \bar{U}^2 \Lambda^2 \frac{d^2 \varphi}{dx^2} + \left( \frac{R}{Z_J} \cos \varphi + \frac{Z_J}{R_J} \right) \bar{U} \Lambda \frac{d\varphi}{dx} \\ = -\frac{1}{2} \sin \varphi_1 (\varphi_1 - \varphi) (\varphi - \varphi_2). \end{aligned} \quad (57)$$

For qualitative analysis of (54) when the first two terms in the l.h.s. of the equation are comparable, it is better to present it as a system of two first order differential equations

$$\begin{aligned} \left[ \frac{\cos \varphi}{12} + \left( \frac{C_J}{C} + \frac{R}{R_J} \right) \bar{U}^2 \right] \Lambda \frac{d\chi}{dx} = \frac{\sin \varphi}{12} \chi^2 \\ - \left( \frac{R}{Z_J} \cos \varphi + \frac{Z_J}{R_J} \right) \bar{U} \chi - \sin \varphi + \bar{U}^2 \varphi + F, \end{aligned} \quad (58a)$$

$$\Lambda \frac{d\varphi}{dx} = \chi, \quad (58b)$$

Now, one important feature of shocks can be understood immediately. We are talking about the direction of shock propagation. Linearising Eq. (58) in the vicinity

of the fixed points  $(\chi, \varphi) = (0, \varphi_1)$  and  $(\chi, \varphi) = (0, \varphi_2)$  we obtain

$$\Lambda \begin{pmatrix} d\chi/dx \\ d\varphi/dx \end{pmatrix} = \begin{pmatrix} M_i & N_i \\ 1 & 0 \end{pmatrix} \begin{pmatrix} \varphi - \varphi_i \\ \chi \end{pmatrix}, \quad i = 1, 2 \quad (59)$$

where

$$M_i = - \left( \frac{R}{Z_J} \cos \varphi_i + \frac{Z_J}{R_J} \right) \bar{U}, \quad (60a)$$

$$N_i = \frac{\bar{U}^2 - \cos \varphi_i}{\cos \varphi_i / 12 + (C_J/C + R/R_J) \bar{U}^2}. \quad (60b)$$

The eigenvalues of the matrix in (59) are

$$\lambda_{i,\pm} = \frac{M_i \pm \sqrt{M_i^2 + 4N_i}}{2}. \quad (61)$$

Thus negative  $N_i$  corresponds to a stable fixed point, and positive  $N_i$  – to a semi-stable fixed point. From the fact that  $\varphi_1$  is a semi-stable fixed point, and  $\varphi_2$  is a stable fixed point we obtain

$$\cos \varphi_2 > \bar{U}_{\text{sh}}^2(\varphi_1, \varphi_2) > \cos \varphi_1. \quad (62)$$

The inequalities (62) allow only one direction of shock propagation - from smaller  $\cos \varphi$  to larger  $\cos \varphi$ . Taking into account (28), we can present (62) as

$$\bar{u}^2(\varphi_2) > \bar{U}_{\text{sh}}^2(\varphi_1, \varphi_2) > \bar{u}^2(\varphi_1), \quad (63)$$

thus establishing the connection with the well known in the nonlinear waves theory fact: the shock velocity is higher than the sound velocity in the region before the shock but lower than the sound velocity in the region behind the shock<sup>1</sup>.

Let us write down inequalities (62) explicitly

$$\cos \varphi_2 > \frac{\sin \varphi_1 - \sin \varphi_2}{\varphi_1 - \varphi_2} > \cos \varphi_1. \quad (64)$$

We will combine the case we studied up to now, when  $\varphi_1$  was the phase before the shock and  $\varphi_2$  - behind the shock, with the opposite case, which corresponds to indices 1 and 2 in (64) being interchanged. The points in the phase space of the shock boundary conditions  $(\varphi_1, \varphi_2)$ , for which neither (64), nor its interchanged version are satisfied, and hence the shock is forbidden, can be visualized by the fact that the secant of the curve  $\sin \varphi$  between the points crosses the curve, like it is shown on Fig. 5 (above). Because  $\sin \varphi$  is concave downward for  $0 < \varphi < \pi/2$ , and concave upward for  $-\pi/2 < \varphi < 0$ , the shock is allowed between any pair of  $\varphi_1, \varphi_2$  having the same sign. For  $\varphi_1$  and  $\varphi_2$  having opposite signs the shock may be allowed or not. We present the phase space of shock boundary conditions on Fig. 5 (below). The forbidden region is shaded.

When the asymptotic phases on the two sides of the JTL belong to the shaded region, probably the forbidden

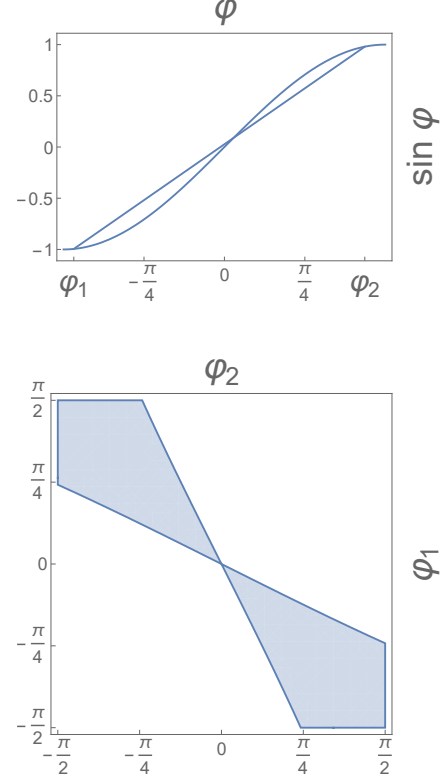


FIG. 5: (above): The geometric property of the points belonging to the shaded region. (below): The phase space of the boundary conditions on the ends of the JTL  $\varphi_1$  and  $\varphi_2$ . The region, which corresponds to the forbidden shock boundary conditions, is shaded.

shock is split into two allowed ones: between  $\varphi_1$  and some intermediate  $\varphi_{in}$ , and between  $\varphi_2$  and  $\varphi_{in}$ . Say, when  $\varphi_2 = -\varphi_1$ , the system may chose the intermediate value  $\varphi_{in} = 0$ . In this hypothetical case, the shocks move in the opposite directions, and the central part with the phase  $\varphi_{in} = 0$  expands with the velocity  $2U_k(\varphi_1, 0)$ . However, the case of multiple shocks, being simultaneously present in the system, demands further studies.

## B. The numerical integration

Equation (54) can be easily integrated numerically in the general case. For aesthetical reasons let us simplify it by putting  $R = 0$  and  $C_J = 0$ . (Actually, the physical meaning and the relevance of the resistor in series with the ground capacitor is not obvious. We included it because we were able to do it for free. The capacitance of the JJ is certainly physically relevant. Anyhow, when  $C_J/C \ll 1$ , it can be ignored.) After the simplification and substitution of the results for  $\bar{U}$  and  $F$  from (12) and

(17), the equation becomes

$$\frac{\Lambda^2}{12} \frac{d^2 \sin \varphi}{dx^2} + \frac{Z_J}{R_J} \bar{U}_{\text{sh}}(\varphi_1, \varphi_2) \Lambda \frac{d\varphi}{dx} = \frac{(\varphi - \varphi_2)(\sin \varphi_1 - \sin \varphi) - (\sin \varphi - \sin \varphi_2)(\varphi_1 - \varphi)}{\varphi_1 - \varphi_2}. \quad (65)$$

The result of the numerical integration of (65) is shown on Fig. 6 (compare with Figs. 2 (below)).

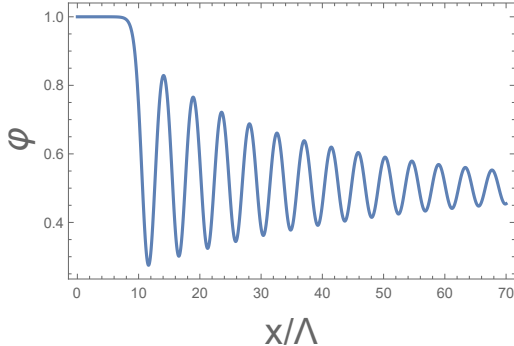


FIG. 6: The shock profile according to Eq. (65). We have chosen  $\varphi_1 = 1$ ,  $\varphi_2 = .5$ ,  $Z_J/R_J = .005$ .

Dissipation is always present in real experiments. And yet we can observe solitary waves (though they are non-stationary, but practically identical to the corresponding stationary solitons at any given moment of time) in case if dissipation is weak enough. Looking at Fig. 6 we realize that weak dissipation does not completely kill solitary waves, it just makes them nonstationary/attenuating. Such solitary waves are observed in numerical calculations and in experiments, as was the case with granular chains<sup>41,43</sup>. On the other hand, there is a critical rate of dissipation which transforms oscillating stationary shock waves into monotonous<sup>48</sup>. This also can be seen from Eq. (61).

### C. The simple wave approximation

If we return to Eq. (53), discard the running wave ansatz, assume that  $R = 0$  and  $C_J = 0$  and assume the dissipation to be small we obtain instead of (42)

$$\left( \frac{\partial}{\partial \tau} - \frac{\sqrt{L_J/C}}{2R_J} \frac{\partial^2}{\partial z^2} \right)^2 \varphi = \left( \frac{\partial}{\partial z} + \frac{1}{24} \frac{\partial^3}{\partial z^3} \right)^2 \sin \varphi. \quad (66)$$

Extracting root square from both parts of (66) we obtain the generalization of (45)

$$\frac{\partial \varphi}{\partial \tau} = \pm \left( \frac{\partial \varphi}{\partial z} - \frac{1}{12} \frac{\partial \varphi^3}{\partial z} + \frac{1}{24} \frac{\partial^3 \varphi}{\partial z^3} \right) + \frac{\sqrt{L_J/C}}{2R_J} \frac{\partial^2 \varphi}{\partial z^2}, \quad (67)$$

and the generalization of (48)

$$\begin{aligned} \frac{\partial \psi}{\partial \tau} = & \pm \sqrt{\cos \varphi_1} \left( \frac{\partial \psi}{\partial z} - \frac{\tan \varphi_1}{4} \frac{\partial \psi^2}{\partial z} + \frac{1}{24} \frac{\partial^3 \psi}{\partial z^3} \right) \\ & + \frac{\sqrt{L_J/C}}{2R_J} \frac{\partial^2 \psi}{\partial z^2}, \end{aligned} \quad (68)$$

which is KdV equation with dissipation<sup>1</sup>.

## VIII. DISCUSSION

Recently, quantum mechanical description of JTL in general and parametric amplification in such lines in particular started to be developed, based on quantisation techniques in terms of discrete mode operators<sup>49</sup>, continuous mode operators<sup>50</sup>, a Hamiltonian approach in the Heisenberg and interaction pictures<sup>51</sup>, the quantum Langevin method<sup>52</sup>, or on partitions a quantum device into compact lumped or quasi-distributed cells<sup>53</sup>. It would be interesting to understand in what way the results of the present paper are changed by quantum mechanics. Particularly interesting looks studying of quantum ripples over a semi-classical shock<sup>54</sup> and fate of quantum shock waves at late times<sup>55</sup>. Closely connected problem of classical and quantum dispersion-free coherent propagation in waveguides and optical fibers was studied recently in Ref.<sup>56</sup>.

Finally, we would like to express our hope that the results obtained in the paper are applicable to kinetic inductance based traveling wave parametric amplifiers based on a coplanar waveguide architecture. Onset of shock-waves in such amplifiers is an undesirable phenomenon. Therefore, shock waves in various JTL should be further studied, which was one of motivations of the present work.

## IX. CONCLUSIONS

We have analytically studied the localized running waves in the discrete Josephson transmission lines (JTL), constructed from Josephson junctions (JJ) and capacitors. The quasi-continuum approximation reduces calculation of the running wave profiles to the problem of equilibrium of an elastic rod in the potential field. Making additional approximation, we reduced the problem to the motion of the fictitious Newtonian particle in the potential well and calculated the velocities and the profiles of the kinks and the solitons. We have found that the nonstationary smooth waves which are small perturbations on the non-zero background can be described by the Korteweg-de Vries equation, and those on zero background – by modified Korteweg-de Vries equation. We also studied the effect of dissipation on the running waves in JTL and find that in the presence of the resistors, shunting the JJ and/or in series with the ground capac-

itors, the only possible stationary running waves are the shock waves, whose profiles are also found.

### Acknowledgments

The main idea of the present work was born in the discussions with M. Goldstein. We are also grateful to J. Cuevas-Maraver, A. Dikande, M. Inc, P. Kevrekidis, B. A. Malomed, V. Nesterenko, T. H. A. van der Reep, and B. Ya. Shapiro for their comments (some of which were crucial for the completion of the project) and to P. Rosenau for his criticism.

### Appendix A: Propagator for the linear transmission line

In this Section we consider the transmission line, obtained from that presented on Fig. 1, by substituting linear inductor for the JJ. The circuit equations are

$$L \frac{dI_n}{dt} = \frac{1}{C} (q_{n+1} - 2q_n + q_{n-1}), \quad (\text{A1a})$$

$$\frac{dq_n}{dt} = I_n, \quad (\text{A1b})$$

where  $I_n$  is the current,  $C$  is the capacitance, and  $L$  is the inductance. Eliminating  $I_n$  and introducing the dimensionless time  $\tau = t/\sqrt{LC}$  we obtain

$$\frac{d^2q_n(\tau)}{d\tau^2} = q_{n+1}(\tau) - 2q_n(\tau) + q_{n-1}(\tau). \quad (\text{A2})$$

Because the system is linear (but dispersive), it doesn't allow either kinks or solitary waves, and thus seems to lie outside the scope of the paper. However, we'll use the system to check up the modified quasi-continuum approximation, which Section VI we apply to the JTL.

#### 1. The exact solution

We define the propagator by the initial and the boundary conditions

$$q_n(0) = \delta_{n0}, \quad \dot{q}_n(0) = 0, \quad (\text{A3a})$$

$$\lim_{n \rightarrow \pm\infty} q_n = 0. \quad (\text{A3b})$$

Recalling the recurrence relation satisfied by Bessel functions<sup>57</sup>

$$2 \frac{dZ_n(\tau)}{d\tau} = Z_{n-1}(\tau) - Z_{n+1}(\tau), \quad (\text{A4})$$

where  $Z$  is any Bessel function, and repeating it twice we obtain

$$4 \frac{d^2Z_n(\tau)}{d\tau^2} = Z_{n+2}(\tau) - 2Z_n(\tau) + Z_{n-2}(\tau). \quad (\text{A5})$$

Comparing (A5) with (A2) we obtain plausible solution for half of the problem. This solution – for even  $n$  – is

$$q_n(\tau) = J_{2n}(2\tau), \quad (\text{A6})$$

where  $J_n$  is the Bessel function of the first kind.

To obtain a rigorous solution (and for the whole problem) we use Laplace transformation

$$Q_n(s) = \int_0^\infty d\tau e^{-s\tau} q_n(\tau). \quad (\text{A7})$$

For  $Q_n(s)$  we obtain the difference equation

$$Q_{n+1}(s) - (2 + s^2)Q_n(s) + Q_{n-1}(s) = -s\delta_{n0}. \quad (\text{A8})$$

Solving (A8) we get

$$Q_n(s) = \frac{1}{\sqrt{s^2 + 4}} \left( \frac{\sqrt{s^2 + 4} - s}{2} \right)^{2|n|}. \quad (\text{A9})$$

Taking into account the inverse Laplace transform correspondence tables<sup>57</sup>, we obtain Eq. (A6) for all  $n$ .

Though we will not use the following result, consider the signalling in the discrete semi-infinite linear transmission line. The problem is characterized by Eq. (A2) for  $n \geq 1$  with the initial and the boundary conditions

$$q_n(0) = \dot{q}_n(0) = 0, \quad (\text{A10a})$$

$$q_0(\tau) = \delta(\tau), \quad \lim_{n \rightarrow +\infty} q_n(\tau) = 0. \quad (\text{A10b})$$

The problem can be solved exactly. After Laplace transformation we obtain difference equation

$$Q_{n+1}(s) - (2 + s^2)Q_n(s) + Q_{n-1}(s) = 0 \quad (\text{A11})$$

with the boundary conditions

$$Q_0(s) = 1, \quad \lim_{n \rightarrow +\infty} Q_n(\tau) = 0. \quad (\text{A12})$$

Solving (A11) we get

$$Q_n(s) = \left( \frac{\sqrt{s^2 + 4} - s}{2} \right)^{2n}. \quad (\text{A13})$$

Taking into account the inverse Laplace transform correspondence tables<sup>57</sup>, we obtain<sup>45,58</sup>

$$q_n(\tau) = \frac{2n}{\tau} J_{2n}(2\tau). \quad (\text{A14})$$

#### 2. The modified quasi-continuum approximation

Now let us solve the problem approximately. We'll consider  $q$  as a function of the continuous variable  $z = n$  (for simplicity in this Section and in the next one we put

$\Lambda = 1$ ), and present the r.h.a. of Eq. (A2) modifying the quasi-continuum approximation (18) to

$$q_{n+1}(\tau) - 2q_n(\tau) + q_{n-1}(\tau) = \left( \frac{\partial}{\partial z} + \frac{1}{24} \frac{\partial^3}{\partial z^3} \right)^2 q. \quad (\text{A15})$$

We will call (A15) the modified quasi-continuum approximation. After that, (A2) is decoupled into two equations for right and left going waves

$$\frac{\partial q}{\partial \tau} = \pm \left( \frac{\partial q}{\partial z} + \frac{1}{24} \frac{\partial^3 q}{\partial z^3} \right). \quad (\text{A16})$$

The propagator is defined by the initial and the boundary conditions

$$q(z, 0) = \delta(z), \quad \lim_{z \rightarrow \pm\infty} q(z, \tau) = 0. \quad (\text{A17})$$

Making Laplace transformation with respect to  $\tau$  and Fourier transformation with respect to  $z$

$$\mathcal{Q}(k, s) = \int_0^\infty d\tau e^{-s/\tau} \int_{-\infty}^{+\infty} dz q(z, \tau) e^{ikz}, \quad (\text{A18})$$

we obtain for the right going part of the propagator the equation

$$\left( s - ik + \frac{ik^3}{24} \right) \mathcal{Q}(k, s) = 1. \quad (\text{A19})$$

Solving Eq. (A19) we get

$$\mathcal{Q}(k, s) = \frac{1}{s - ik + \frac{ik^3}{24}}. \quad (\text{A20})$$

Making the inverse Laplace and Fourier transformations we obtain

$$\begin{aligned} q(z, \tau) &= \frac{1}{4\pi} \int_{-\infty}^{+\infty} dk \exp[i(\tau - z)k - i\tau k^3/24] \\ &= \tau^{-1/3} \text{Ai} \left[ 2\tau^{-1/3}(z - \tau) \right], \end{aligned} \quad (\text{A21})$$

where  $\text{Ai}$  is the Airy function<sup>57</sup>. Equation (A21) describes the signal front at  $z \sim \tau/2$ , exponentially small precursor for  $\tau < 2z$ , and oscillations and power law decrease of the signal in the wake for  $\tau > 2z$ . The width of the transition region between the two asymptotic forms increases with time as  $\tau^{1/3}$ .

Fig. 7 compares Eq. (A21) with the exact result (A6) for  $\tau$  from zero up to a couple of  $z$ . To compare the results for  $\tau \gg z$ , we may use asymptotic forms of Bessel and Airy functions<sup>57</sup>

$$J_{2n}(2\tau) \sim \sqrt{\frac{1}{\pi\tau}} (-1)^n \cos \left( 2\tau - \frac{\pi}{4} \right), \quad (\text{A22a})$$

$$\tau^{-1/3} \text{Ai} \left[ 2\tau^{-1/3}(z - \tau) \right] \sim \sqrt{\frac{1}{\pi\tau}} \cos \left[ A\tau \left( 1 - \frac{z}{\tau} \right)^{3/2} - \frac{\pi}{4} \right], \quad (\text{A22b})$$

where  $A = 2^{5/2}/3 \approx 1.9$ .

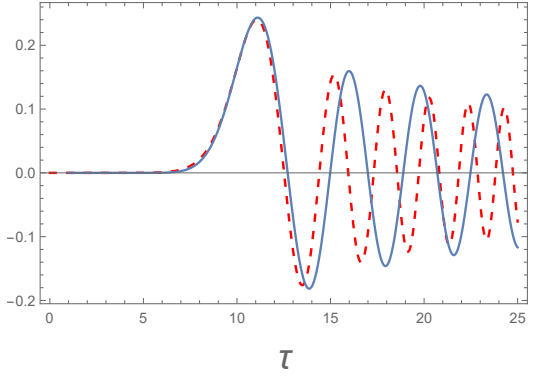


FIG. 7: Propagator calculated for  $n = 10$  exactly (Eq. (A6), solid blue line) and for  $z = 10$  in the framework of the modified quasi-continuum approximation (Eq. (A21), dashed red line).

## Appendix B: The integral approximation: the kinks

In this Appendix we are looking for some way to approximate the finite difference in the r.h.s. of Eq. (1a) alternative to Taylor expansion (13). We were not able to advance far on the road we have taken here (if at all). However, some equations obtained in the process look quite amusing to us, and we decided to present them to general attention.

Treating  $\varphi$  and  $q$  as functions of the continuous variable  $z$  (which we measure in  $\Lambda$ ), let us approximate the finite difference in the r.h.s. of Eq. (1a) as

$$q_{n+1} - 2q_n + q_{n-1} = \int_{-\infty}^{+\infty} dz' g(z - z') \frac{d^2 q(z', \tau)}{dz'^2}, \quad (\text{B1})$$

where  $g(z)$  is a non-singular function, which is positive, even and has the following zero and second moments

$$\int_{-\infty}^{+\infty} dz g(z) = 1, \quad (\text{B2a})$$

$$\int_{-\infty}^{+\infty} dz z^2 g(z) = \frac{\Lambda^2}{6}, \quad (\text{B2b})$$

Looking for the running wave (7) solution of (1), we obtain the integro-differential equation for the function  $\varphi(x)$

$$\bar{U}^2 \frac{d\varphi(x)}{dx} = \int_{-\infty}^{+\infty} dx' \frac{dg(x - x')}{dx} \sin \varphi(x'). \quad (\text{B3})$$

Integrating Eq. (B3) with respect to  $x$  we obtain nonlinear Fredholm integral equations of the second kind<sup>60</sup>

$$\bar{U}^2 \varphi(x) = \int_{-\infty}^{+\infty} dx' g(x - x') \sin \varphi(x') - F. \quad (\text{B4})$$

Imposing the boundary conditions (8) and going to the limits  $x \rightarrow +\infty$  and  $x \rightarrow -\infty$ , we recover Eq. (16) and,

hence, (12) and (17). Substituting  $\bar{U}^2$  and  $F$  into Eq. (B4) we get the counterpart of Eq. (25) (or (20))

$$\begin{aligned}\varphi(x) = & \frac{\varphi_1 - \varphi_2}{\sin \varphi_1 - \sin \varphi_2} \int_{-\infty}^{+\infty} dx' g(x - x') \sin \varphi(x') \\ & + \frac{\varphi_2 \sin \varphi_1 - \varphi_1 \sin \varphi_2}{\sin \varphi_1 - \sin \varphi_2}.\end{aligned}\quad (\text{B5})$$

Now let us consider Eq. (B5) per se, forgetting the properties of  $\varphi(x)$  which were postulated to derive it. We realise that if  $\varphi(x)$  goes to some limits when  $x \rightarrow +\infty$  and  $x \rightarrow -\infty$ , each of these limits is either  $\varphi_1$ , or  $\varphi_2$ . This is unfortunately all we can say about the solution. Previously we have seen that Eq. (25) (or (20)) has solution only if  $\varphi_2 = -\varphi_1$ . We are unable to prove that for Eq. (B5). However, if the relation  $\varphi_2 = -\varphi_1$  is imposed, Eq. (B5) takes the form

$$\varphi(x) = \frac{\varphi_1}{\sin \varphi_1} \int_{-\infty}^{+\infty} dx' g(x - x') \sin \varphi(x'). \quad (\text{B6})$$

The only thing we can prove about the solution of Eq. (B6) is that, for any  $x$ ,

$$-\varphi_1 \leq \varphi(x) \leq \varphi_1 \quad (\text{B7})$$

(for the sake of definiteness we consider  $\varphi_1$  to be positive). In fact, let  $\sin \varphi(x)$  reaches maximum value at some point  $x_0$ , and  $\sin \varphi(x_0) > \sin \varphi_1$ . Then

$$\begin{aligned}& \frac{\varphi_1}{\sin \varphi_1} \int_{-\infty}^{+\infty} dx' g(x_0 - x') \sin \varphi(x') \\ & < \frac{\varphi_1}{\sin \varphi_1} \sin \varphi(x_0) < \varphi_0\end{aligned}\quad (\text{B8})$$

(in the last step we took into account that  $\sin \varphi/\varphi$  decreases when  $\sin \varphi$  increases for positive  $\varphi$ ). So we came to a contradiction. Similar for the minimum value of  $\sin \varphi$ .

---

\* Electronic address: Eugene.Kogan@biu.ac.il

<sup>1</sup> G. B. Whitham, *Linear and Nonlinear Waves*, John Wiley & Sons Inc., New York (1999).

<sup>2</sup> D. M. French and B. W. Hoff, IEEE Trans. Plasma Sci. **42**, 3387 (2014).

<sup>3</sup> B. Nouri, M. S. Nakhla, and R. Achar, IEEE Trans. Microw. Theory Techn. **65**, 673 (2017).

<sup>4</sup> L. P. S. Neto, J. O. Rossi, J. J. Barroso, and E. Schamiloglu, IEEE Trans. Plasma Sci. **46**, 3648 (2018).

<sup>5</sup> M. S. Nikoo, S. M.-A. Hashemi, and F. Farzaneh, IEEE Trans. Microw. Theory Techn. **66**, 3234 (2018); **66**, 4757 (2018).

<sup>6</sup> L. C. Silva, J. O. Rossi, E. G. L. Rangel, L. R. Raimundi, and E. Schamiloglu, Int. J. Adv. Eng. Res. Sci. **5**, 121 (2018).

<sup>7</sup> Y. Wang, L.-J. Lang, C. H. Lee, B. Zhang, and Y. D. Chong, Nat. Comm. **10**, 1102 (2019).

<sup>8</sup> E. G. L. Range, J. O. Rossi, J. J. Barroso, F. S. Yamasaki, and E. Schamiloglu, IEEE Trans. Plasma Sci. **47**, 1000 (2019).

<sup>9</sup> A. S. Kyuregyan, Semiconductors **53**, 511 (2019).

<sup>10</sup> N. A. Akem, A. M. Dikande, and B. Z. Essimbi, SN Applied Science **2**, 21 (2020).

<sup>11</sup> A. J. Fairbanks, A. M. Darr, A. L. Garner, IEEE Access **8**, 148606 (2020).

<sup>12</sup> R. Landauer, IBM J. Res. Develop. **4**, 391 (1960).

<sup>13</sup> S. T. Peng and R. Landauer, IBM J. Res. Develop. **17** (1973).

<sup>14</sup> M. I. Rabinovich and D. I. Trubetskoy, *Oscillations and Waves*, Kluwer Academic Publishers, Dordrecht / Boston / London (1989).

<sup>15</sup> B. D. Josephson, Phys. Rev. Lett. **1**, 251 (1962).

<sup>16</sup> A. Barone and G. Paterno, *Physics and Applications of the Josephson Effect*, John Wiley & Sons, Inc, New York (1982).

<sup>17</sup> N. F. Pedersen, Solitons in Josephson Transmission lines, in *Solitons*, North-Holland Physics Publishing, Amsterdam (1986).

<sup>18</sup> C. Giovanella and M. Tinkham, *Macroscopic Quantum Phenomena and Coherence in Superconducting Networks*, World Scientific, Frascati (1995).

<sup>19</sup> A. M. Kadin, *Introduction to Superconducting Circuits*, Wiley and Sons, New York (1999).

<sup>20</sup> M. Remoissenet, *Waves Called Solitons: Concepts and Experiments*, Springer-Verlag Berlin Heidelberg GmbH (1996).

<sup>21</sup> O. Yaakobi, L. Friedland, C. Macklin, and I. Siddiqi, Phys. Rev. B **87**, 144301 (2013).

<sup>22</sup> K. O'Brien, C. Macklin, I. Siddiqi, and X. Zhang, Phys. Rev. Lett. **113**, 157001 (2014).

<sup>23</sup> C. Macklin, K. O'Brien, D. Hover, M. E. Schwartz, V. Bolkhovsky, X. Zhang, W. D. Oliver, and I. Siddiqi, Science **350**, 307 (2015).

<sup>24</sup> B. A. Kochetov, and A. Fedorov, Phys. Rev. B **92**, 224304 (2015).

<sup>25</sup> A. B. Zorin, Phys. Rev. Applied **6**, 034006 (2016); Phys. Rev. Applied **12**, 044051 (2019).

<sup>26</sup> D. M. Basko, F. Pfeiffer, P. Adamus, M. Holzmann, and F. W. J. Hekking, Phys. Rev. B **101**, 024518 (2020).

<sup>27</sup> T. Dixon, J. W. Dunstan, G. B. Long, J. M. Williams, Ph. J. Meeson, C. D. Shelly, Phys. Rev. Applied **14**, 034058 (2020).

<sup>28</sup> A. Burshtein, R. Kuzmin, V. E. Manucharyan, and M. Goldstein, Phys. Rev. Lett. **126**, 137701 (2021).

<sup>29</sup> T. C. White et al., Appl. Phys. Lett. **106**, 242601 (2015).

<sup>30</sup> A. Miano and O. A. Mukhanov, IEEE Trans. Appl. Supercond. **29**, 1501706 (2019).

<sup>31</sup> Ch. Liu, Tzu-Chiao Chien, M. Hatridge, D. Pekker, Phys. Rev. A **101**, 042323 (2020).

<sup>32</sup> P. Rosenau, Phys. Lett. A **118**, 222 (1986); Phys. Scripta **34**, 827 (1986).

<sup>33</sup> G. J. Chen and M. R. Beasley, IEEE Trans. Appl. Supercond. **1**, 140 (1991).

<sup>34</sup> H. R. Mohebbi and A. H. Majedi, IEEE Trans. Appl. Supercond. **19**, 891 (2009); IEEE Transactions on Microwave Theory and Techniques **57**, 1865 (2009).

<sup>35</sup> A. Houwe, S. Abbagari, M. Inc, G. Betchewe, S. Y. Doka, K. T. Crepin, and K. S. Nisar, *Results in Physics* **18**, 103188 (2020).

<sup>36</sup> H. Katayama, N. Hatakenaka, and T. Fujii, *Phys. Rev. D* **102**, 086018 (2020).

<sup>37</sup> D. L. Sekulic, N. M. Samardzic, Z. Mihajlovic, and M. V. Sataric, *Electronics* **10**, 2278 (2021).

<sup>38</sup> P. G. Kevrekidis, I. G. Kevrekidis, A. R. Bishop, and E. Titi, *Phys. Rev. E*, **65**, 046613 (2002).

<sup>39</sup> L. Q. English, F. Palmero, A. J. Sievers, P. G. Kevrekidis, and D. H. Barnak, *Phys. Rev. E*, **81**, 046605 (2010).

<sup>40</sup> P. G. Kevrekidis, *IMA Journal of Applied Mathematics* **76**, 389 (2011)

<sup>41</sup> V. Nesterenko, *Dynamics of heterogeneous materials*, Springer Science & Business Media (2013).

<sup>42</sup> B. A. Malomed, *The sine-gordon model: General background, physical motivations, inverse scattering, and solitons*, The Sine-Gordon Model and Its Applications. Springer, Cham, 1-30 (2014).

<sup>43</sup> V. F. Nesterenko, *Phil. Trans. R. Soc. A* **376**, 20170130 (2018).

<sup>44</sup> B. A. Malomed, *Nonlinearity and discreteness: Solitons in lattices*, Emerging Frontiers in Nonlinear Science. Springer, Cham, 81 (2020).

<sup>45</sup> E. Kogan, *Journal of Applied Physics* **130**, 013903 (2021).

<sup>46</sup> I. Roy, S.V. Dmitriev, P.G. Kevrekidis, A. Saxena, *Phys. Rev. E* **76**, 026660 (2007).

<sup>47</sup> L.D. Landau, E. M. Lifshitz, A. M. Kosevich, and L. P. Pitaevskii, *Theory of elasticity: (Vol. 7)*, Elsevier (1986).

<sup>48</sup> E. B. Herbold and V. F. Nesterenko, *Phys. Rev E*, **75**, 021304, (2007).

<sup>49</sup> T. H. A. van der Reep, *Phys. Rev. A* **99**, 063838 (2019).

<sup>50</sup> L Fasolo, A Greco, E Enrico, in *Advances in Condensed-Matter and Materials Physics: Rudimentary Research to Topical Technology*, (ed. J. Thirumalan and S. I. Pokutny), Scence (2019).

<sup>51</sup> A. Greco, L. Fasolo, A. Meda, L. Callegaro, and E. Enrico, *Phys. Rev. B* **104**, 184517 (2021).

<sup>52</sup> Y. Yuan, M. Haider, J. A. Russer, P. Russer and C. Jirauschek, 2020 XXXIIrd General Assembly and Scientific Symposium of the International Union of Radio Science, Rome, Italy (2020).

<sup>53</sup> Z. K. Minev, Th. G. McConkey, M. Takita, A. D. Corcoles, and J. M. Gambetta, arXiv:2103.10344 (2021).

<sup>54</sup> E. Bettelheim and L. I. Glazman, *Phys. Rev. Lett.* **109**, 260602 (2012).

<sup>55</sup> Th. Veness and L. I. Glazman, *Phys. Rev. B* **100**, 235125 (2019).

<sup>56</sup> A. Mandilara, C. Valagiannopoulos, and V. M. Akulin, *Phys. Rev. A* **99**, 023849 (2019).

<sup>57</sup> M. Abramowitz, I. A. Stegun eds., *Handbook of Mathematical Functions with Formulas, Graphs, and Mathematical Tables*, (National Bureau of Standards, Washington, 1964).

<sup>58</sup> N. Kwidzinski and R. Bulla, arXiv:1608.0061.

<sup>59</sup> P. G. Drazin, R. S. Drazin, *Solitons: an introduction* (Vol. 2), Cambridge university press (1989).

<sup>60</sup> A. M. Wazwaz, *Linear and nonlinear integral equations*, Berlin: Springer (2011).